European Journal of Neuroscience (2008) 28(9):1731-1742.

Differential changes in axonal conduction following CNS demyelination in two mouse models.

Bando Y, Takakusaki K, Ito S, Terayama R, Kashiwayanagi M, Yoshida S.

Differential changes in axonal conduction following central nervous system demyelination in two mouse models.

Yoshio Bando[1,4], Kaoru Takakusaki[2,4], Shinji Ito[1], Ryuji Terayama[1,3], Makoto Kashiwayanagi[2], and Shigetaka Yoshida[1]

[1]Department of functional anatomy and Neuroscience and [2]Department of functional neurophysiology, Asahikawa Medical College, Midorigaoka-Higashi 2-1-1-1, Asahikawa, Hokkaido 078-8510, [3]Department of Oral Function and Anatomy, Okayama University Graduate School of Medicine, Dentistry and Pharmaceutical Sciences, 2-5-1 Shikata-cho, Okayama 700-8525, JAPAN, [4]These authors equally contributed to this work.

Abbreviated title: myelination and nerve conduction

Key Words: oligodendrocytes, nerve conduction, myelin

Total number of words in this paper: 7,340 words
(Abstract: 250 words, Introduction: 462 words)

40 pages, 9 figures and 2 tables

Address correspondence to: Yoshio Bando, Ph.D
Department of functional anatomy and neuroscience, Asahikawa Medical College, Midorigaoka-Higashi 2-1-1-1, Asahikawa, Hokkaido 078-8510, JAPAN
Phone: +81-166-68-2303, Fax: +81-166-68-2309
E-mail: ybando@asahikawa-med.ac.jp

Abstract

Transgenic and disease model mice have been used to investigate the molecular mechanisms of demyelinating diseases. However, less attention has been given to elucidating changes in nerve conduction in these mice. We established an experimental system to measure the response latency of cortical neurons and examined changes in nerve conduction in cuprizone-induced demyelinating mice and in myelin basic protein-deficient *shiverer* mice. Stimulating and recording electrodes were placed in the right and left sensori-motor cortices respectively. Electrical stimulation of the right cortex evoked antidromic responses in left cortical neurons with a latency of 9.38 ± 0.31 ms (N=107; mean ± SEM). While response latency was longer in mice at 7 days and 4 weeks of cuprizone treatment (12.35 ± 0.35 ms; N=102, 11.72 ± 0.29 ms; N=103, respectively), response latency at 7 days and 4 weeks after removal of cuprizone was partially restored (10.72 ± 0.45 ms; N=106 and 10.27 ± 0.34 ms; N=107, respectively). Likewise, electron microscopy showed cuprizone-induced demyelination in the corpus callosum and nearly complete remyelination after cuprizone removal. We also examined whether the myelin abnormalities in *shiverer* mice affected their response latencies. But there were no significant differences in response latencies in *shiverer* (9.83 ± 0.24 ms; N=103) and wild type (9.33 ± 0.22 ms; N=112) mice. The results of these

electrophysiological assessments imply that different demyelinating mechanisms, differentially affecting axon conduction, are present in the cuprizone-treated and *shiverer* mice, and may provide new insights to understanding the pathophysiology of demyelinatation in animal models in the CNS.

Introduction

Oligodendrocytes (OLGs) form myelin sheaths in the central nervous system (CNS) and are important for nerve conduction. The myelin wraps around axons and facilitates the rapid, salutatory conduction of electrical impulses along them (Morell et al., 1999). OLGs are vulnerable to a variety of insults, including proteases and inflammatory cytokines (Ledeen et al., 1998: Link, 1998). The destruction of OLGs results in the loss of both myelin and nerve conduction. For example, oligodendroglial loss is implicated in the onset of multiple sclerosis (MS), an inflammatory demyelinating disease of the human CNS. Previous studies reported oligodendroglial cell death in MS plaques, suggesting that nerve conduction in MS patients is slowed by demyelination accompanying oligodendroglial loss (Dowling et al., 1997).

Apoptotic OLGs are observed in spinal cords of rodents with experimental autoimmune encephalomyelitis (EAE), a recognized animal model for MS (Terayama et al., 2005; Hisahara et al., 2001; Raine, 1997). Demyelination and axonal loss are also associated with electrophysiological abnormalities in spinal cords of mice with EAE (Lo et al., 2003: McGavern et al., 2000). However, little attention has been given to investigating the electrophysiological changes occurring during demyelination or remyelination in the brain.

We previously reported that oligodendroglial apoptosis is induced by cuprizone, followed by demyelination in the corpus callosum (Bando et al., 2006). Our findings are consistent with other reports that cuprizone induces demyelination that appears to be reversible upon discontinuation of the cuprizone treatment (Arnett et al. 2001; Gao et al. 2000; Blakemore 1972; Ludwin 1978; Komoly et al. 1992; Komoly et al. 1987; Kim et al. 1991). Therefore this experimental model is useful for examining nerve conduction during demyelination and remyelination.

MBP is a major component of the myelin sheath. Mutations in this gene, which can be observed in *shiverer* mice, disrupt myelination (Chernoff 1981). The *shiverer* mutation is autosomal recessive and is characterized by the onset of tremors about the 12^{th} days after birth, seizures at later times, and a progressive deterioration ending in an early death (Chernoff 1981: Uschlureit et al., 2000: Seiwa et al., 2002). The CNS of a *shiverer* mutant mouse is almost entirely devoid of myelin membranes. Axons of a *shiverer* mouse may be ensheathed by multiple lamellae of OLGs processes, but myelin is not uniformly compacted. Moreover axoglial junctions are irregular in shape, size, and distribution (Kandel et al., 1995; Seiwa et al., 2002; Rosenbluth 1980, 1981; Inoue et al., 1981). Therefore, *shiverer* mice were used as a comparison to clarify the effects of abnormal myelin on nerve conduction.

Therefore, it is not clear whether changes in nerve conduction caused by oligodendroglial loss actually occur in these experimental models. To answer this question, we examined nerve conduction in the callosal connections of cuprizone (bis-cyclohexanon oxaldihydrazone)-induced demyelinated mice and myelin basic protein (MBP)-deficient *shiverer* mice.

Materials and Methods

Animals.

BALB/c mice and *shiverer* mice (6-8 weeks old) were used in this study. *Shiverer* mice (B6 strain; $shi^{-/-}$, Molineaux et al., 1986) were recovered from frozen eggs kindly supplied by Dr. M. Kimura (Tokai Univ., Japan) and Dr. M. Yokoyama (Mitsubishi Kasei Institute of Life Science, Japan). *Shiverer* mice were selected from crossings of heterozygous animals ($shi^{+/-}$). These mice were maintained and propagated by mating in the Animal Institute of Asahikawa Medical College. All experimental protocols were carried out according to the guidelines laid down by the NIH in the US regarding the care and use of animals for experimental procedures, and to protocols approved by the institutional animal care and use committee of Asahikawa Medical College. Every attempt was made to minimize animal suffering and to reduce the number of mice used. We also used another *shiverer* mouse (C3H strain) obtained from The Jackson Laboratory. Results of experiments with these two strains were similar.

Genotyping.

Genotyping of the wild-type ($shi^{+/+}$) and *shiverer* mice ($shi^{-/-}$) was performed by PCR on DNA isolated from tail samples. Deletions in the MBP gene (exon II to VII)

were verified by PCR using synthesized oligonucleotide primers hybridizing to a 5' intron sequence upstream of the deleted exon II, 5' primer: GAGGCCGCACATCAGCCCTGATTTTTG CTAAG, and a corresponding 3' primer: CATGTATGAATGTGCATCTTGGGCAAT CTATCT.

Induction of demyelination and remyelination.

Mouse chow containing 0.7% bis-cyclohexanone-oxaldihydrazone (cuprizone; Sigma, St. Louis, Missouri) was synthesized (Oriental Yeast Co. LTD, Chiba, Japan). To introduce demyelination, mice were fed mouse chow containing 0.7% cuprizone for 7 days. Remyelination was initiated by returning the mice to a normal diet for another 7 days (Nihon SLC Co. LTD, Shizuoka, Japan) after 7 days of cuprizone treatment (Bando et al., 2006). In a chronic model, mice were fed mouse chow containing 0.7% cuprizone for the first 7 days and then that containing 0.2% cuprizone for 3 weeks (total: 4 weeks treatment). Chronic demyelination with a diet containing 0.2% cuprizone has been reported (Skiripuletz et al., 2008: Irvine and Blakemore, 2008: Franco-Pons et al., 2007). Remyelination in chronically-treated mice was initiated by returning them to a normal diet (Nihon SLC Co. LTD, Shizuoka, Japan) for 1 week to 4 weeks.

Surgery and electrophysiological recording

Mice were anesthetized with a mixture of xylazine and ketamine (100 and 10 mg/kg, respectively; i.p.) and fixed in a streotaxic frame (Tanaka et al., 2004). Additional doses of anesthesia as above were administrated to maintain a suitable level of anesthesia. Body temperature was maintained between 35.0~37.0 °C using heat radiant ramps, and care was taken not to induce bleeding when the skull was drilled. Tungsten stimulating (concentric electrode with a tip diameter 0.1 mm, Eiko-Kagaku, Co., Tokyo, JAPAN) and recording needle electrodes (monopolar electrodes with a tip diameter of 10 μm, Eiko-Kagaku, Co., Tokyo) were placed in the right and left sensori-motor cortices, respectively, according to the coordinates of The mouse brain (Academic press, FL, USA, stim: 2.0 mm posterior and 1.5 mm lateral to bregma; rec: 2.0 mm posterior and 1.5 mm lateral to bregma. See Fig. 2A). The activities of cortical neurons antidromically stimulated (rectangular pulses of <200 μA, 0.2 ms, 1 Hz to the right sensory-motor cortex) via the callosal connection were amplified by a biophysical amplifier (ER-1, Cygnas, Co. PA, USA) with a high-pass filter (10 ms time constant), monitored using an oscilloscope, and recorded. The data were stored in a personal computer using the PowerLab software system (PowerLab/16SP, AD Instruments, Nagoya, JAPAN).

Injection of fluorogold

To first examine the distribution of cortical neurons driven via callosal connections following stimulation of the contralateral sensori-motor cortex, mice were injected, under anesthesia (as above), with the retrograde tracer fluorogold in a modified version of the protocol described previously (Yamada et al., 2006). In brief, 5 μl of fluorogold solution diluted in saline were injected via a Hamilton syringe placed at the same location as the stimulating electrode. After injection, the lesions were closed, and 2 days later the brains were removed and prepared for hematoxy-eosin (HE) staining.

Tissue preparation.

Mice were anesthetized with pentobarbital sodium (Nembutal, 100 mg/kg, i.p.) and perfused transcardially with saline followed by 4% paraformaldehyde in 0.1 M phosphate buffer (PB, pH 7.4). Brains were removed, postfixed overnight in the same fixative, and then immersed in 30% sucrose in 0.1 M PB for 1-2 days. Brains were then frozen in powdered dry ice, embedded in OCT (Tissue-Tek), and stored at –80 ˚C prior to staining (Bando et al., 2006).

HE staining and LFB staining

Frozen 14 μm-thick coronal sections of brain were cut on a cryostat and mounted onto silane-coated slides (Matsunami, Japan). The sections were stained with hematoxilin and eosin and analyzed with a light microscope (ECLIPSE 80i; Nikon, Japan). In some experiments, the sections were stained with Luxol Fast Blue/cresyl violet (LFB/CV), demonstrating myelination as described previously (Terayama et al., 2005).

Immunohistochemisty

Frozen 14 μm-thick coronal sections of brain obtained from *shiverer* mice were cut on a cryostat and stained with mouse monoclonal anti-MBP antibody (Chemicon; 1:1000) and anti-glutathione-S-transferase-π (GST-π) antibody (BD biosci., Tokyo, Japan; 1:125) as previously described (Bando et al., 2006). Anti-GST-π antibody was used as a marker of mature oligodendrocytes (Tansey et al., 1991). Briefly, sections were incubated overnight with anti-MBP antibody or anti-GST-π antibody at 4°C. Avidin-biotin conjugated secondary antibody was used to visualize primary antibody binding (Vectastain® Elite ABC: Vector Laboratories Inc., Burlingam, CA) as previously described (Onuki et al., 2004; Bando et al., 2005).

Electron Microscopy

Mice were transcardially perfused with 2% glutaraldehyde and 2% paraformaldehyde in 0.1 M PB. Brains were removed, fixed with 1% osmium tetroxide and embedded in Epon. Ultrathin sections were cut and stained with uranyl acetate and lead citrate and observed with a transmission electron microscope (EM, H-7650).

Statistical analyses

Data are expressed as means ± SEM. Experimental groups were compared by Mann-Whiteney's U test or ANOVA followed by Scheffe's F test. Values of $p<0.05$ were considered significant.

Results

Distribution of neurons antidromically stimulated via the callosal connections

To first examine the possible distribution of neurons antidromically stimulated from the right sensori-motor cortex, mice were injected with fluorogold. Labeled cells were distributed specifically in the left cerebral hemisphere in a very restricted region of sensori-motor cortex (Fig. 1A and B). HE staining also showed that neurons labeled by fluorogold were cortical neurons (Fig. 1C). These results aided in the placement of recording electrodes at a very restricted region where fluorogold-labeled cells were observed. Stimulating and recording electrodes in the right and left sensori-motor cortices, respectively, were placed at a distance of 3.0 mm from one another (Fig. 2A).

Recording antidromic responses of cortical neurons

Following stimulation of the right sensori-moter cortex, extracellular activities were recorded from the left sensori-moter cortex at various depths from 0 μm to 900 μm from the surface (Fig. 2B). The stimulation evoked a mixture of extracellular field potentials and action potentials of cortical neurons (Fig. 2C). These potentials were most prominent at depths of 0.2~0.3 mm and 0.7 mm, which corresponded largely to layers II~III and V, respectively.

Representative examples of antidromic responses obtained in wild type Balb/c mice are shown in Figure 3. A cortical neuron recorded at a depth of 280 μm was located in layer III (Figure 3A) Single pulse stimulation (50 μA) induced action potentials with a fixed latency of 12.4 ms and an amplitude of 0.5 mV (Fig.3Ai). Because the twin action potentials evoked by twin pulses of stimuli exhibited the same fixed latencies, we judged this neuron to be antidromically activated by the stimuli (Fig.3Aii). The neuron in Fig.3B was recorded at a depth of 710 μm (layer V), and exhibited action potentials with amplitudes of 3.0 mV following single stimuli. Although this cell was activated by contralateral cortical stimuli (70 μA), the latencies of action potentials fluctuated, suggesting that they were synaptically evoked by the stimuli (Fig.3Bi). By increasing the stimulus current to 80 μA, action potentials with fixed latencies of 0.85 ms were evoked by either single or twin pulses (Fig.3Bii and 3Biii).

To accurately measure the conduction times of cortical neurons activated via callosal connections, we collected only those cortical neurons (n=740) that displayed antidromic responses (fixed latencies after stimulation). Because such neurons with callosal connections (callosal neurons) were located predominantly in layers II-III and V, we divided cortical neurons into two groups depending on the depth at which they were

recorded: neurons recorded not deeper than 400 μm, which included the layer II-III neurons, and those recorded deeper than 400 μm, which included the layer V neurons. The amplitudes of action potentials recorded from deep layer neurons to be larger than those of the more superficial layer neurons (Fig. 2C and Fig. 3). Moreover, the antidromic latencies were significantly shorter in the deep layer neurons than in the superficial layer neurons in the control mice (Table 1).

Distributions of antidromic latency and recorded depth of callosal neurons in cuprizone-induced demyelinating model

Electrophysiological analyses were carried out with control mice (control), mice at 7 days of cuprizone treatment (acute demyelination; cuprizone 7d), at 4 weeks of cuprizone treatment (chronic demyelination; cuprizone 4w), at 7 days after remyelination (Recovery 7d) and at 4 weeks after remyelination (Recovery 4w). Although stimulating and recording electrodes were similarly placed in all mice, mean latencies of antidromically-evoked action potentials were different among these groups (Fig. 4A-E, K). In mice receiving cuprizone for seven days or four weeks, the mean antidromic latencies were significantly longer than in the control mice. Also in mice recovering from this treatment for seven days or four weeks, the mean antidromic

latencies were still significantly longer than in the control mice (Fig. 4K). However, it should be noted that the latencies in both groups of recovering mice were significantly shorter than in those treated with cuprizone for seven days. These findings suggest that axonal conduction in callosally projecting neurons is disturbed by treatment with cuprizone, and that the conduction recovered partly, but not completely, after removal of cuprizone. There were no significant differences in latencies between mice treated for seven days and those treated for four weeks; nor between those recovering for seven days or 4 weeks (Fig. 4K, N).

Among the five groups of mice, callosal neurons were recorded at depths of between 10 μm and 876 μm from the pial surface (Fig. 4F-J). There were no significant differences in the mean depths of the recorded neurons among these groups (Fig. 4L). However, as in the preliminary experiment, extracellular activities with antidromic responses were consistently recorded predominantly at depths of 200-400 μm and 500-700 μm (Fig. 4F-J). As these obviously represented two different populations, we classified callosal neurons into two populations: those in the superficial (≤ 400 μm) and deep (> 400 μm from the surface) layers of the cortex, and compared antidromic latencies or conduction times of callosal neurons in the superficial and the deep layers among the five groups of mice. No significant differences in mean latencies were

observed in superficial layer neurons among the five groups (Fig. 4M and Table 1). By contrast, antidromic latencies of deep layer neurons were significantly different. Namely, the latencies in the demyelinated mice were significantly longer than in controls, and those in the recovering mice significantly shorter than in the demyelinated mice (Fig. 4N and Table 1).

In the present study, data in each group were obtained from four different mice, so inter-animal variations in antidromic response latencies (Fig. 5A) and depths of recorded responses (Fig. 5B) were also examined in each group. There were no inter-animal variations in either the mean latencies or mean depths of callosal neurons, indicating the reproducibility of findings obtained from individual animals in each group.

Morphological changes of myelin in cuprizone-induced demyelination and remyelination

To examine changes in myelin in the demyelinating and remyelinating mice, light microscopic and electron microscopic (EM) studies were carried out. While myelin was well-stained with LFB/CV in control mice (Fig. 6A), deficits in LFB/CV staining were clearly observed as early as three days (Fig. 6B) and more so at seven days (Fig.

6C) of cuprizone treatment. The deficits in LFB/CV staining were far fewer in mice returned to a normal diet after seven days of cuprizone treatment (Fig. 6D), indicating that axons were remyelinated. Essentially the same findings were obtained at the EM level (Fig. 7). While tightly packed, myelin-wrapped axons were clearly seen in control mice (Fig. 7A), there were many myelin-free axons in the corpus callosum of mice treated for 7 days with cuprizone (Fig. 7B). On the other hand, most axons were wrapped with myelin at 7 days after removal of cuprizone (Fig. 7C), but these axons were thinly wrapped with myelin compared with controls (Fig. 7A and C).

Morphological changes in myelin of *shiverer* mice

As a comparison of myelin-deficient models, we also examined nerve conduction in myelin deficient-*shiverer* mice. As shown in Fig. 8A, immunoblot analysis demonstrated that heterozygous mice expressed MBP protein in the cerebellum, cerebrum and spinal cord. By contrast, expression of MBP protein was not observed in these regions in shiverer mice. No anti-MBP staining was observed in the corpus callosum of *shiverer* mice (Fig. 8B), but GST-π immunoreactive OLGs were observed (Fig. 8C). These results suggest that maturation of OLGs was not inhibited in the *shiverer* mice, whereas the expression of MBP protein was suppressed. EM analyses of

these mice yielded results consistent with previous reports (Kandel et al., 1995; Readhead et al., 1987); presence of greatly deficient and abnormal myelin in *shiverer* mice (Fig. 8E) compared with control mice (Fig. 8D).

Characteristics of callosal neurons in *shiverer* mice

Finally, we examined the antidromic response latency of callosal neurons in wild type and *shiverer* mice. In both groups, the antidromic response latencies of most neurons were distributed between 5 and 15 ms. There was no significant difference in mean latencies of the shiverer and wild type mice (Figs. 9A, B, and E). By contrast, there *was* a significant difference in the depths at which antidromically activated neuronal responses were recorded (Fig. 9C, D, and F). In wild type mice, the antidromic responses were mostly obtained at less than 400 μm beneath the brain surface, while in *shiverer* mice, these responses were mainly detected at 400 μm or deeper. Nevertheless, the mean latencies of antidromic responses were not significantly different in the superficial layer ($\leq$400μm) and deep layer (>400 μm) neurons of either group (Fig. 9G and Table 2).

Discussion

Our examination of the effects of demyelination on axonal conduction in cortical neurons innervated via callosal projections from the contralateral cortex can be summarized as follows. First, in general, compared to control mice, the mean conduction time of all callosal neurons was longer in mice demyelinated by cuprizone treatment; this was particularly true of those in layer V. Second, removing cuprizone for as long as four weeks only partially restored the mean conduction time of all neurons. Third, the conduction time of callosal neurons in *shiverer* mice was not significantly changed compared to wild type mice.

While many studies have investigated conduction velocities (CVs) in larger animals, such as monkeys (Evarts, 1965), cats (Takakusaki et al. 2005; Takakusaki et al., 2004) and rats (Takakusaki et al., 1997; Takakusaki and Kitai 1997; Alstermark et al., 2004), there have been few studies on CVs in smaller animals such as mice (Tanaka et al., 2004; Alstermerk et al., 2004). Recently, Tanaka et al. (2004, 2006) examined CVs and relative refractory periods in major tracts (e.g., dorsal column, vestibulospinal, reticulospinal, and corticospinal) of the spinal cord in $plp^{tg/-}$ mice. In addition, McGavern et al. (2000) and Lo et al. (2003) demonstrated, using elegant electrophysiological experiments, that demyelination and axonal loss in the spinal cord

in EAE-treated mice were closely associated with decreased CVs and correlated with the severity of clinical scores. As far as we know, however, less attention has been devoted to examining nerve conduction in the brains of small animal disease models. Thus, we developed an experimental system in mice and investigated nerve conduction of callosal neurons in the animal models of cuprizone-induced demyelination and MBP-deficient *shiverer* mice. The advantages of method are as follows: 1) ease of surgery, including the prevention of bleeding and hypothermia and 2) yields reproducible findings without inter-animal variations within treatment groups.

Cuprizone-induced demyelination resulted in increased conduction times that were only partially reversible following removal of the cuprizone. Histological changes in demyelination and remyelination were correlated with those in antidromic response latencies in these mice. The increased response latency of callosal neurons in the cuprizone-treated mice should reflect a decrease in conduction velocity of demyelinating axons. However, even after 4 weeks of recovery time, the mean antidromic response latencies were only partly restored (Fig. 4). Then what is the mechanism of insufficient recovery of nerve conduction? It was reported that cuprizone-induced demyelination of axons in the corpus callosum was associated with a loss of oligodendroglia, and remyelination was initiated by removal of cuprizone

(Blackmore, 1972: Bando et al., 2006), and we also reported that expression of MBP mRNA recovered to control levels after removal of cuprizone (Bando et al., 2006). The results of our LFB/CV staining (Fig. 6B,C) and electron microscopy (Fig. 7B,C) in the present study are consistent with these observations. However, the *recovered* axons seen by EM seemed to be only loosely wrapped with myelin compared to the controls. Rosenbluth (1980, 1981) hypothesized that conduction velocities may depend more on the degree of ensheathing by multiple lamellae of OLG processes than on the compactness of the myelin. The present results led us to propose that insufficient ensheathing by OLGs or thinly wrapped myelin was responsible for the incomplete recovery of antidromic response latencies, thus, lending support to Rosenbluth's hypothesis.

Another factor contributing to decreased CVs during demyelination is the size of axons. Callosally projecting neurons are primary located in layers III and V (Ivy & Killackey, 1981; Hattox & Nelson, 2007). Pyramidal neurons located in layer V send extensive projections to the striatum, the thalamus and the pyramidal tract on its way to the brainstem and spinal cord in addition to the contralateral cortex (Hattox and Nelson, 2007; Landry et al., 1984; Reiner et al., 2003). Most cortical neurons recorded at 400 μm or less were located in layers I-III and projected to the contralateral cortex through

the corpus callosum (callosal-connected neurons). Moreover, cortical neurons those recorded at 400 μm and deeper are considered as neurons in the layers IV-VI which includes both callosal neurons and corticofugal neurons. In cuprizone-treated mice, changes in the antidromic response latencies were significantly different between deep layer neurons and superficial layer neurons (Figs. 4M-N). Namely, while cuprizone had no significant effects on the layer II-III neurons, antidromic response latencies of the deep layer neurons were significantly lengthened by cuprizone-treatment and were partly restored after removal of cuprizone. These findings suggest that callosal axons of deep layer neurons were more prone to demyelinated by cuprizone. What possible distinguishing features could contribute to these differences between superficial and deep layer neurons? As shown in Table 1, axonal conduction of deep layer neurons was significantly faster than that of superficial layer neurons in control mice, indicating that cell size (or axon diameter) of deep layer neurons were larger than those of the superficial layer neurons, since cell size (or axon diameter) generally correlates with its conduction velocity. Because a larger surface area of multiple lamellae of OLG processes is required to sufficiently ensheath large axons compared to small axons, one possible explanation of the above findings is that the effects of insufficient OLG is more easily seen in large axons than in thin axons.

The results obtained from the *shiverer* mice raise quite an interesting question: why were the response latencies in the *shiverer* mice not significantly different from those in the wild type mice (Figs. 9A-B and G)? These results indicate that the shivering observed in *shiverer* mouse is not caused by alterations in callosal nerve conduction. Rasband et al. (1999) reported that there were far fewer Na^+ channel clusters in the optic nerves of *shiverer* mice than in littermate controls, and that those clusters that did form were often highly irregular. They also showed that distributions of ankyrin-3/G, an attractive candidate for the clustering of Na^+ channels (Srinivasan et al., 1992: Zhou et al., 1998), in adult *shiverer* mice were disrupted and did not form any structures that could be identified as nodes of Ranvier (Rasband et al., 1999). In addition, Sinha et al. (2006) reported that spinal cord axons in *shiverer* mice exhibited dispersed distributions of K^+ channel subunits Kv1.1 and Kv1.2, with a loss of the characteristic distribution of the juxtaparanodal and paranodal areas. Although any one of these abnormalities might be expected to contribute to altered axonal conduction, our study demonstrated that in sensori-motor cortex, there were no differences in the antidromic response latencies between the wild type and *shiverer* mice (Fig. 9).

Our EM study revealed that most callosal axons in the *shiverer* mice were not wrapped by myelin, and even in axons that were wrapped, the myelin was not compact

(Fig. 8E). These results suggest that myelin is not essential for the rapid salutatory conduction in callosal fibers. The clusters of ion channels and myelin may not be the most important factor for producing maximized CVs, once action potential firing has occurred in the brain. For example, densities of Na^+ and K^+ channel clusters did not correlate with CVs during the progression of demyelination (Tanaka et al., 2006: Deerink et al., 1997: Lambert et al., 1997).

In *shiverer* mice, most sensori-motor cortical neurons with antidromic responses were recorded in deep layers of the cortex. By contrast, antidromic responses were recorded predominantly in superficial layers in wild type mice (Fig. 9E-F). This was due to the fact that, unlike in cuprizone-induced demyelinated mice, it was difficult to find cortical neurons with antidromic responses in superficial layers in *shiverer* mice. Based on these results, we hypothesize that it is feasible that corticocortical (layers II-III) and corticofugal (layers IV-VI) networks in *shiverer* mice are different from those in wild types, and that OLG of *shiverer* mice may assist in maintaining their nerve conduction, both of which may contribute to the motor deficit in *shiverer* mice. It has been shown that MBP is associated with visual cortex plasticity (Jiang and Yin, 2007) and myelin is involved in stabilizing neuronal connections by suppressing sprouting and fiber growth (Vanek et al., 1998). Therefore, myelin is important for the development of

cortical neuronal circuits in the critical period. Thus, understanding the essential role of myelin in the development of neuronal networks in *shiverer* mice will be useful for elucidating the mechanisms of motor deficits in these mice.

The present findings also lead us to hypothesize that OLG themselves can contribute to controlling CV. An important difference between cuprizone-treated mice and *shiverer* mice is whether oligodendroglial loss has occurred or not. While cuprizone treatment resulted in considerable oligodendroglial loss (Bando et al. 2006), there was no apparent oligodendroglial loss in *shiverer* mice. OLG may play a protective role for neurons and axons. There are important studies supporting our above hypothesis that OLG dysfunction leads to massive axonal degeneration (Griffiths et al. 1998; Lappe-Siefke et al. 2003; Yin et al. 2006; Simons & Trajkovic 2006). Further study will be helpful to verify this hypothesis.

In conclusion, the present experimental procedures will contribute to understanding the pathophysiological mechanisms of demyelination in the CNS of small animal models of disease. The present study also suggests that OLG themselves, in the absence of compact myelin, may play a critical role in maintaining rapid salutatory conduction.

Acknowledgements

This work was supported by grants from the Ministry of Education, Science, Culture and Sports of Japan (to S.Y., Y.B. and K.T.), the Inamori Foundation (to S.Y.), the Noastec (to S.Y.), the Akiyama Foundation (to Y.B.), The Osaka Medical Foundation for Incurable Diseases (to Y.B.), and a Grant-in-Aid for Scientific Research on Priority Areas (Area # 454) from the Japanese Ministry of Education, Culture, Sports, Science and Technology (to K.T.)**.** We thank K. Hazawa and T. Sasaki (Dept. of Functional Anatomy and Neuroscience, Asahikawa Medical College) for their technical support. We also thank N. Shimizu, T. Hayakawa, and K. Nakaya (Animal Institute of Asahikawa Medical College) for maintaining and propagating the Balb/c mice and *shiverer* mice.

Abbreviations:

CNS; central nervous system, CVs; conduction velocities, EAE; experimental autoimmune encephalomyelitis; EM; electron microscope, GST-π; Pi-form of glutathione-S-transferase, MBP; myelin basic protein, MS; multiple sclerosis, OLGs; oligodendrocytes, PLP; proteolipid protein

References

Alstermark B, Ogawa J & Isa T (2004) Lack of monosynaptic corticomotoneuronal EPSPs in rats: disynaptic EPSPs mediated via reticulospinal neurons and polysynaptic EPSPs via segmental interneurons. J. Neurophysiol. 91, 1832–1839.

Arnett HA, Mason J, Marino M, Suzuki K, Matsushima GK & Ting JP (2001) TNF alpha promotes proliferation of oligodendrocyte progenitors and remyelination. Nat Neurosci. 11, 1116-1122.

Bando Y, Ito S, Nagai Y, Terayama R, Kishibe M, Jiang YP, Mitrovic B, Takahashi T & Yoshida S (2006) Implications of protease M/neurosin in myelination during experimental demyelination and remyelination. Neurosci. Lett. 405, 175-180.

Bando Y, Onuki R, Katayama T, Manabe T, Kudo T, Taira K & Tohyama M (2005) Double-strand RNA dependent protein kinase (PKR) is involved in the extrastriatal degeneration in Parkinson's disease and Huntington's disease. Neurochem. Int. 46, 11-18.

Blackmore WF (1972) Observations on oligodendrocyte degeneration, the resolution of status spongiosus and remyelination in cuprizone intoxication in mice. J. Neurocyrol. 1, 413-426.

Chernoff GF (1981) Shiverer: an autosomal recessive mutant mouse with myelin deficiency. J Hered. 72 (2), 128.

Dowling P, Husar W, Menonna J, Donnenfeld H, Cook S & Sidhu M (1997) Cell death and birth in multiple sclerosis brain. J Neurol Sci. 149 (1), 1-11.

Deerinck TJ, Levinson RS, Bennett VG & Ellisman MH (1997) Clustering of voltage-sensitive sodium channels on axons is independent of direct Schwann cell contact in the dystrophic mouse. J Neurosci 17, 5080–5088.

Evarts EV (1965) Relation of discharge frequency to conduction velocity in pyramidal tract neurons. J. Neurophysiol. 28, 216–228.

Franco-Pons N, Torrente M, Colomina MT & Vilella E (2007) Behavioral deficits in the cuprizone-induced murine model of demyelination/remyelination. Toxicol Lett. 169(3), 205-13.

Gao X, Gillig TA, Ye P, D'Ercole AJ, Matsushima GK & Popko B (2000) Interferon-γ protects against cuprizone-induced demyelination. Mol. Cell. Neurosci. 16, 338-349.

Griffiths I, Klugmann M, Anderson T, Yool D, Thomson C, Schwab MH, Schneider A, Zimmermann F, McCulloch M, Nadon N (1998) Axonal swellings and degeneration in mice lacking the major proteolipid of myelin. Science 280, 1610-1613.

Hisahara S, Yuan J, Momoi T, Okano H & Miura M (2001) Caspase-11 mediates oligodendrocyte cell death and pathogenesis of autoimmune-mediated demyelination. J Exp Med. 193 (1), 111-122.

Hattox AM & Nelson SB (2007) Layer V neurons in mouse cortex projecting to different targets have distinct physiological properties. J Neurophysiol 98, 3330-3340.

Inoue Y, Nakamura R, Mikoshiba K & Tsukada Y (1981) Fine structure of the central myelin sheath in the myelin deficient mutant Shiverer mouse, with special reference to the pattern of myelin formation by oligodendroglia. Brain Res. 219 (1), 85-94.

Irvine KA & Blakemore WF (2008) Remyelination protects axons from demyelination-associated axon degeneration. Brain. May 18.

IvyGO, Killackey HP (1981) The ontogeny of the distribution of callosal projection neurons in the rat parietal cortex. J Comp Neurol 195, 367-389.

Jiang WS & Yin ZQ (2007) Screening of gene associated with termination of the critical period of visual cortex plasticity in rats. Curr. Eye Research 32, 709-716.

Kandel ER, Schwartz JH & Jessell TM (1995) Essentials of Neuronal Science and Behavior, Appleton & Lange, pp.51-53.

Kim YS & Kim SU (1991) Oligodendroglial cell death induced by oxygen radicals and its protection by catalase. J Neurosci Res. 29 (1), 100-106.

Komoly S, Jeyasingham MD, Pratt OE & Lantos PL (1987) Decrease in oligodendrocyte carbonic anhydrase activity preceding myelin degeneration in cuprizone induced demyelination. J Neurol Sci. 79 (1-2), 141-148.

Komoly S, Hudson LD, Webster HD & Bondy CA (1992) Insulin-like growth factor I gene expression is induced in astrocytes during experimental demyelination. Proc. Natl. Acad. Sci. USA 89, 1894-1898.

Landry P, Wilson CJ & Kitai ST (1984) Morphological and electrophysiological characteristics of pyramidal tract neurons in the rat. Exp Brain Res 57, 177-190.

Lambert S, Davis JQ & Bennett V (1997) Morphogenesis of the node of Ranvier: co-clusters of ankyrin and ankyrin-binding integral proteins define early developmental intermediates. J Neurosci 17, 7025–7036.

Lappe-Siefke C, Goebbels S, Gravel M, Nicksch E, Lee J, Braun PE, Griffiths IR & Nave KA (2003) Disruption of cnp1 uncouples oligodendroglial functions in axonal support and myelination. Nat Genet. 33, 366-374.

Ledeen RW & Chakraborty G (1998) Cytokines, signal transduction, and inflammatory demyelination: review and hypothesis. Neurochem Res. 23 (3), 277-289.

Link H (1998) The cytokine storm in multiple sclerosis. Mult Scler. 4 (1), 12-15.

Lo AC, Saab CY, Black JA & Waxman SG (2003) Phenytoin protect spinal cord axons and preserves axonal conduction and neurological function in a model of neuroinflammation in vivo. J Neurophysiol. 90, 3566-3571.

Ludwin SK (1978) Central nervous system demyelination and remyelination in the mouse: an ultrastructural study of cuprizone toxicity. Lab Invest. 39 (6), 597-612.

McGavern DB, Murray PD, Rivera-Quinones C, Schmelzer JD, Low PA & Rodriguez

M (2000) Axonal loss results in spinal cord atrophy, electrophysiological abnormalities and neurological deficits following demyelination in a chronic inflammatory model of multiple sclerosis. Brain 123, 519-531.

Molineaux SM, Engh H, de Ferra F, Hudson L & Lazzarini RA (1986) Ecombination within the myelin basic protein gene created the dysmyelinating shiverer mouse mutation. Proc Natl Acad Sci USA 83, 7542-7546.

Morell P, Barrett CV, Mason JL, Toews AD, Hostettler JD, Knapp GW & Matsushima GK (1998) Gene expression in brain during cuprizone-induced demyelination and remyelination. Mol Cell Neurosci. 12(4-5), 220-227.

Onuki R, Bando Y, Suyama E, Katayama T, Kawasaki H, Baba T, Tohyama M & Taira K (2004) An RNA-dependent protein kinase is involved in tunicamycin-induced apoptosis and Alzheimer's disease. The EMBO J. 23, 959-968.

Raine CS (1997) The Norton Lecture: a review of the oligodendrocyte in the multiple sclerosis lesion. J Neuroimmunol. 77 (2), 135-52.

Rasband MN, Peles E, Trimmer JS, Levinson SR, Lux SE & Shrager P (1999) Dependence of nodal sodium channel clustering on paranodal axoglial contact in the depeloping CNS. J. Neurosci. 19 (17), 7516-7528.

Reiner A, Jiao Y, Del Mar N, Laverghetta AV & Lei WL (2003) Differential morphology of pyramidal tract-type and intratelencephalically projecting-type corticostriatal neurons and their intrastriatal terminals in rats. J Comp Neurol 457, 420-440.

Rosenbluth J (1980) Central myelin in the mouse mutant shiverer. J Comp Neurol. 194 (3), 639-48.

Readhead C, Popko B, Takahashi N, Shine HD, Saavedra RA, Sidman RL & Hood L (1987) Expression of a myelin basic protein gene in transgenic shiverer mice: Correction of the demyelinating phenotype. Cell 48, 703-712.

Rosenbluth J (1981) Axoglial junctions in the mouse mutant Shiverer. Brain Res. 208 (2), 283-97.

Skripuletz T, Lindner M, Kotsiari A, Garde N, Fokuhl J, Linsmeier F, Trebst C & Stangel M. (2008) Cortical demyelination is prominent in the murine cuprizone model and is strain-dependent. Am J Pathol. 172 (4), 1053-61.

Seiwa C, Kojima-Aikawa K, Matsumoto I & Asou H (2002) CNS Myelinogenesis in Vitro: Myelin Basic Protein Deficient Shiverer OLGs. J. Neurosci. Res. 69, 305-317.

Shinha K, Karimi-Abdolrezaee S, Velumian AA & Fehlings MG (2006) Functional changes in genetically dysmyelinated spinal cord axons of shiverer mice: role of juxtaparanodal Kv1 family K+ channels. J Neurophysiol 95, 1683-1695.

Simons M & Trajkovic K (2006) Neuron-glia communication in the control of oligodendrocyte function and myelin biogenesis. J Cell Sci. 119, 4381-4389.

Srinivasan Y, Lewallen M & Angelides KJ (1992) Mapping the binding site on ankyrin for the voltage-dependent sodium channel from brain. J. Bio. Chem. 267, 7483-7489

Takakusaki K, Shiroyama T & Kitai ST. (1997) Two types of cholinergic neurons in the rat tegmental pedunculopontine nucleus: electrophysiological and morphological characterization. Neuroscience. 79 (4), 1089-1109.

Takakusaki K, Takahashi K, Saitoh K, Harada H, Okumura T, Kayama Y & Koyama Y. (2005) Orexinergic projections to the cat midbrain mediate alternation of emotional behavioural states from locomotion to cataplexy. J Physiol. 568 (Pt 3), 1003-1020.

Takakusaki K, Habaguchi T, Saitoh K & Kohyama J (2004) Changes in the excitability of hindlimb motoneurons during muscular atonia induced by stimulating the pedunculopontine tegmental nucleus in cats. Neuroscience. 124 (2), 467-80.

Takakusaki K & Kitai ST (1997) Ionic mechanisms involved in the spontaneous firing of tegmental pedunculopontine nucleus neurons of the rat. Neuroscience. 78 (3), 771-794.

Tansey FA & Cammer W (1991) A pi form of glutathione-S-transferase is a myelin- and oligodendrocytes-associated enzyme in mouse brain. J. Neurochem. 57(1), 95-102.

Tanaka H, Ono K, Shibasaki H, Isa T & Ikenaka K (2004) Conduction properties of identified neural pathways in the central nervous system of mice in vivo. Neurosci Res. 49(1), 113-22.

Tanaka H, Ikenaka K & Isa T (2006) Electrophysiological abnormality precedes apparent histological demyelination in the CNS of mice over-expressing proteolipid protein. J Neurosci. Res. 84 (6), 1206-16.

Terayama R, Bando Y, Yamada M & Yoshida S (2005) Involvement of neuropsin in the pathogenesis of experimental autoimmune encephalomyelitis. Glia. 52(2), 108-118.

Uschkureit T, Sporkei O, Stracke J, Bussow H & Stoffel, W (2000) Early onset of axonal degeneration in double (plp-/-mag-/-) and hypomyelinosis in triple (plp-/-mbp-/-mag-/-) mutant mice. J Neurosci. 20 (14), 5225-5233.

Vanek P, Thallmair M & Schwab ME (1998) Increased lesion induced sprouting of corticospinal fibers in the myelin free rat spinal cord. Eur. J Neurosci., 10, 45-56.

Yamada M, Terayama R, Bando Y, Kasai S & Yoshida S (2006) Regeneration of the abdominal postganglionic sympathetic system. Neurosci Res. 54(4), 261-268.

Yin X, Baek RC, Kirschner DA, Peterson A, Fujii Y, Nave KA, Macklin WB & Trapp BD (2006) Evolution of a neuroprotective function of central nervous system myelin. J Cell Biol. 172, 469-478.

Zhou D, Lambert S, Malen PL, Carpenter S, Boland LM & Bennett V (1998) Ankyrin-G is reqired for clustering of voltage-gated Na channels at axon initial segments and for normal action potential firing. J. Cell Biol. 143, 1295-1304.

Table 1 Antidromic latencies in corpus callosum of cuprizone-treated mice.

Condition	Latency (msec)		p-value
	≤ 400 μm	> 400 μm	
Control	10.31 ± 0.47 (n=51)	8.54 ± 0.38 (n=56)	0.01**
Cuprizone 7 days	11.48 ± 0.45 (n=56)	13.40 ± 0.52 (n=46)	0.01**
Cuprizone 4 wks	11.41 ± 0.36 (n=65)	12.21 ± 0.45 (n=38)	0.23
Recovery 7 days	11.49 ± 0.67 (n=52)	9.99 ± 0.59 (n=54)	0.04*
Recovery 4 wks	10.51 ± 0.47 (n=49)	10.08 ± 0.48 (n=58)	0.32

*p=0.04, **p=0.01 significantly different from ≤400 μm (Mann Whiteney's U test)

Table 2 The antidromic response latencies in cortex of *shiverer* mice.

Condition	Latency (ms)		p-value
	≤ 400 μm	> 400 μm	
wild type (shi+/+)	9.45 ± 0.25 (n=83)	8.92 ± 0.43 (n=35)	0.27
shiverer (shi-/-)	10.14 ± 0.51 (n=32)	9.62 ± 0.25 (n=71)	0.55

Note: There were no significant differences between latencies recorded at >400 μm and those at >400 μm in either group. (Mann Whiteney's U test).

Figure legends

Figure 1. Distribution of cortical neurons targeted by contralateral stimulation via the callosal connection.

(A) Balb/c mice were injected with fluorogold from the left cerebral hemisphere at the point where the stimulating electrode would have been placed. (B) High power magnification of the region with the box in (A). By the fluorogold-stained neurons, we determined where to place the recording electrode. (C) HE staining showing the fluorogold injection site (arrowhead). Scale bars: (A and C) 100 μm and (B) 50 μm.

Figure 2. Recording antidromic responses of cortical neurons in mice

(A) Stimulating (Stim.) and recording (Rec.) electrodes were placed in the right and left sensori-motor cortices, respectively, separated by a distance of 3.0 mm. Electrical stimulation (less than 200 μA, 1 Hz) applied to the right cortex evoked antidromic responses of cortical neurons in the left cortex. (B) The site and depths of recording electrodes (C) Extracellular recordings of antidromic responses in cortical neurons after stimulation at various depths from the pial surface.

Figure 3. Callosally evoked responses of cortical neurons.

(A) Antidoromic responses of a cortical neurons in layer III evoked by single (Ai) and twin (Aii) stimulation pulses. (B) Both orthodromic (Bi,) and antidromic (Bii, iii) responses were recorded in a layer V neuron following 70 μA single and 80 μA single and double stimulation, respectively. Following twin stimulations, antidromic responses exhibit the same latencies after both stimulations.

Figure 4. Distributions of antidromic latencies and recorded depths of callosally innervated neurons in cuprizone-induced demyelinating mice.

(A-E) Distributions of antidromic latencies recorded in mice from the control (A), cuprizone-treated for 7 days (B; cuprizone 7d), cuprizone-treated for 4 weeks (C; cuprizone 4w), remyelination at 7 days (D; recovery 7d) and remyelination at 4 weeks (E; recovery 4w) groups. Mean latencies for each groups are indicated by arrowheads. (F-J) Dot plots showing the relationships between latencies and recording depths in control (F), cuprizone 7d (G), cuprizone 4w (H), recovery 7d (I) and recovery 4w(J) groups. Mean recording depths for each group are shown in each panel (arrowhead), and the dotted lines are at 400 μm. (K). Summary of mean antidromic latencies in each group. (L) Summary of the mean depths of recorded neurons in each group. (M) Mean latencies of neuronal activities recorded at ≤400 μm (layers I-III) in each group. (N)

Mean latencies of neuronal activities recorded at >400 μm (layers IV-IV). Error bars in (K-N) indicate ± SEM. *p<0.05, **p<0.01 significant differences between the indicated groups.

Figure 5. Inter animal variations of the latencies and recording depths

(A) Mean antidromic response latencies of callosal neurons in control (control) and demyelinated (cuprizone 4w) mice. (B) Mean recording depths of antidromic responses in control and demyelinated mice. All data represent means ± SEM. There are no significant differences in either latencies or recording depths among the mice in each group.

Figure 6. Demyelination and remyelination in 0.7% cuprizone-treated mice. Cortical brain sections were stained with luxol fast blue/cresyl biolet (LFB/CV). (A) In untreated control mice, no demyelination is observed in the corpus callosum. (B-D) Time course of demyelination/remyelination during 0.7% cuprizone administration. Brain section at 3 days (B), 7 days (C) and 7 days after removal of cuprizone (D) are shown. Representative sites of demyeliation are indicated by arrowheads. Scale bar: 100 μm.

Figure 7. Morphological changes in myelin in the cuprizone treated mice.

EM analysis of corpus callosum in control (A), at 7 days of cuprizone administration (B), and at 7 days after removal of cuprizone (C). Representative demyelinated axons are indicated with arrowheads. Scale bar: 1 μm

Figure 8. Characterization of myelin-deficient, *shiverer* mice.

(A) Expression of MBP protein in *shiverer* mice was examined by immunoblot analysis. Cerebellum (lane 1), cerebrum (lane 2) and spinal cord (lane 3) from heterozygous (shi+/-) mice. Cerebellum (lanes 4 and 5), cerebrum (lanes 6 and 7) and spinal cord (lanes 8 and 9) from homozygous (shi-/-) mice. (B-C) Immunohistochemistry in *shiverer* mice revealed that, while MBP protein was not detectable (B), GST-π immunoreactive oligodendrocytes were observed in the corpus callosum in *shiverer* mice (C). (D-E) EM analysis of corpus callosum Representative data from control (D) and myelin basic protein (MBP)-deficient *shiverer* (E) mice are shown. Arrowheads in (E) indicate demyelinated axons. Scale bar: 1 μm

Figure 9. Antidromic responses and their recording depths in *shiverer* mice.

(A-B) Distributions of antidromic latencies in wild type (A: open bar) and *shiverer* mice (B: filled bar). Mean latencies are indicated with arrowheads. (C-D) Relationships between the response latencies and their recording depths in wild type ($shi^{+/+}$; C) and *shiverer* ($shi^{-/-}$; D) mice (E) Mean antidromic response latencies and (F) recording depths in wild type ($shi^{+/+}$; open bar) and *shiverer* ($shi^{-/-}$; filled bar) mice (G) Mean response latencies recorded at ≤400 μm or >400 μm Error bars represent ± SEM. **p<0.01 significantly different from

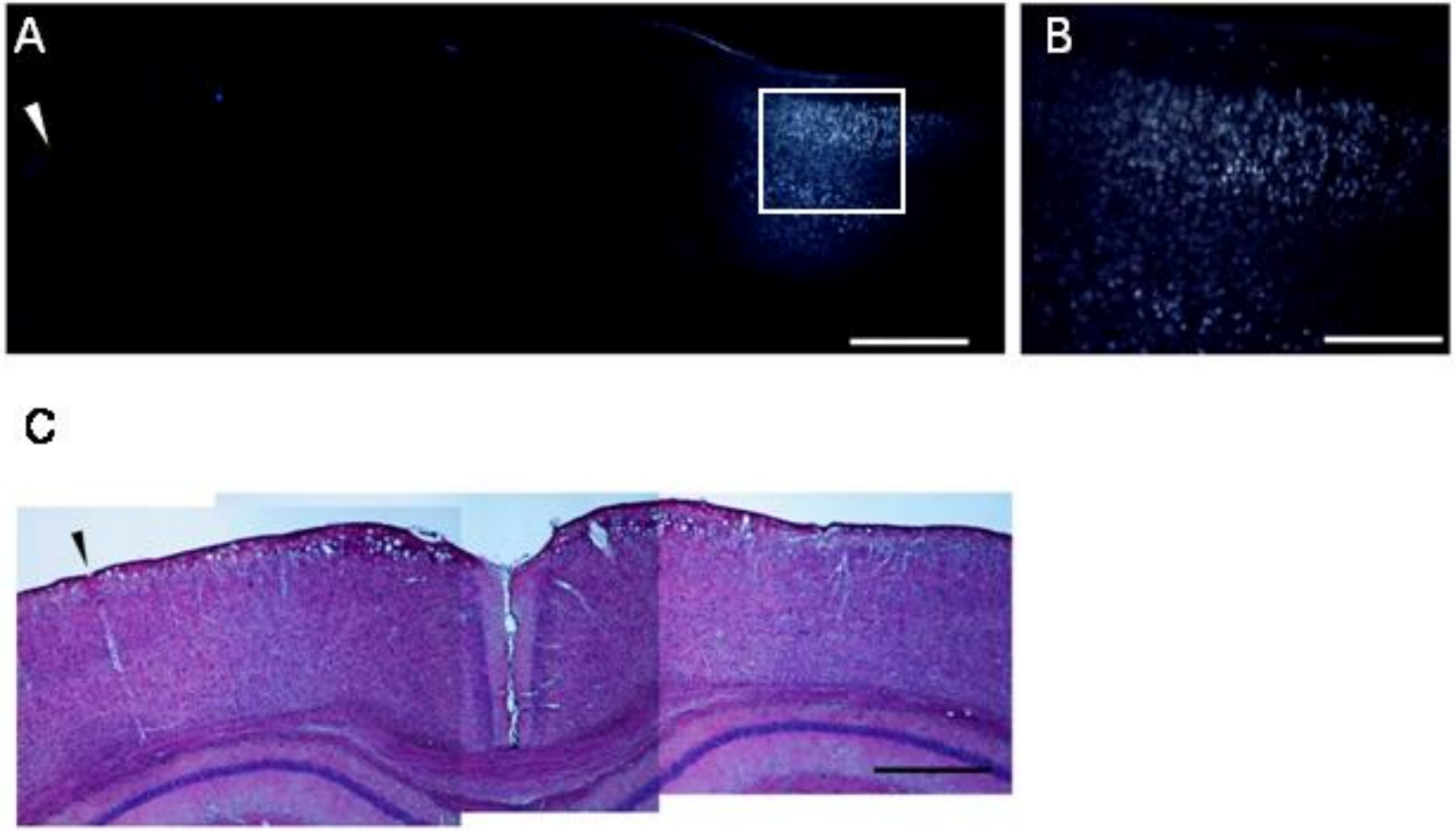

Fig.1 Bando Y. et al.

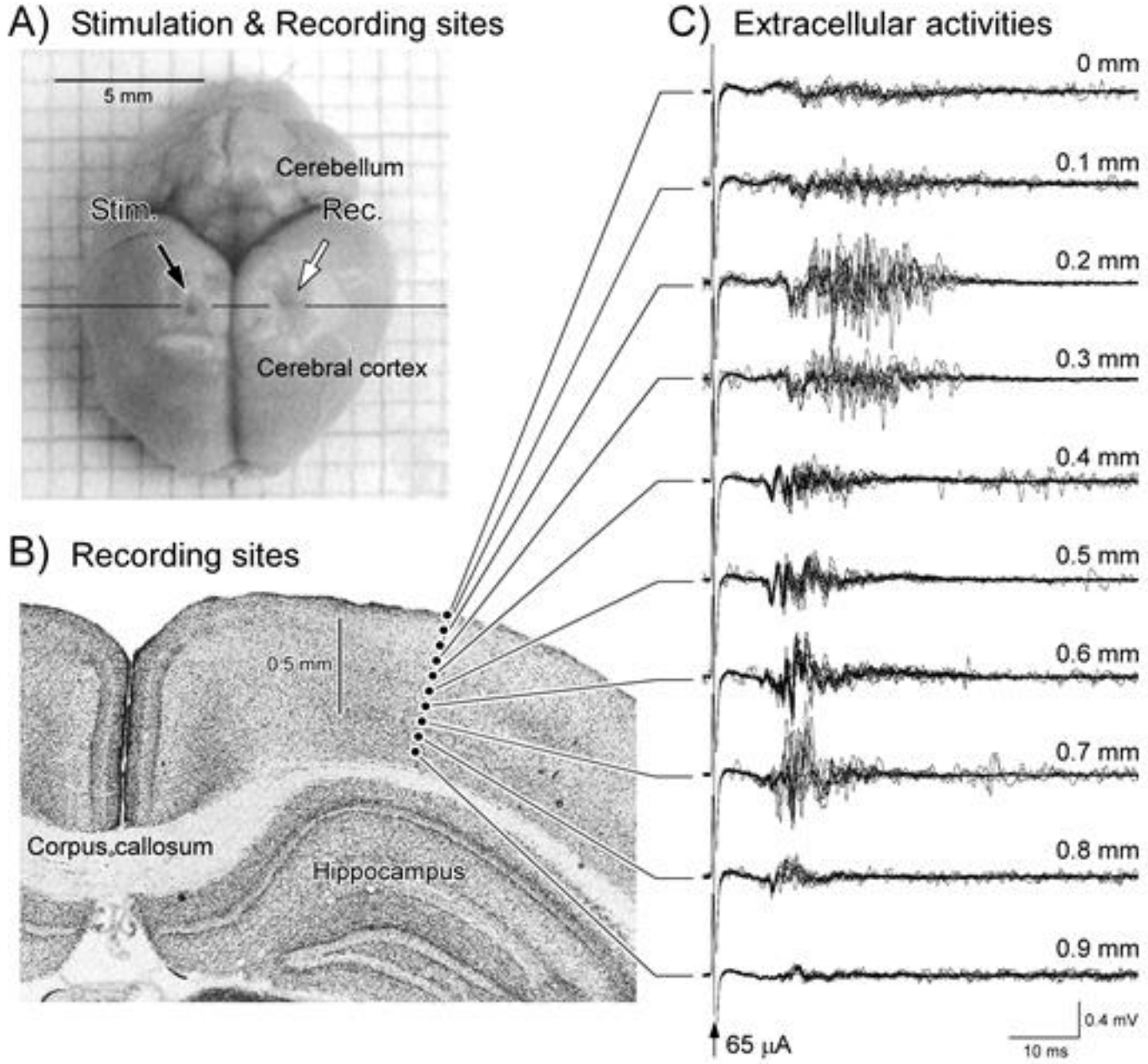

Fig.2 Bando Y et al.

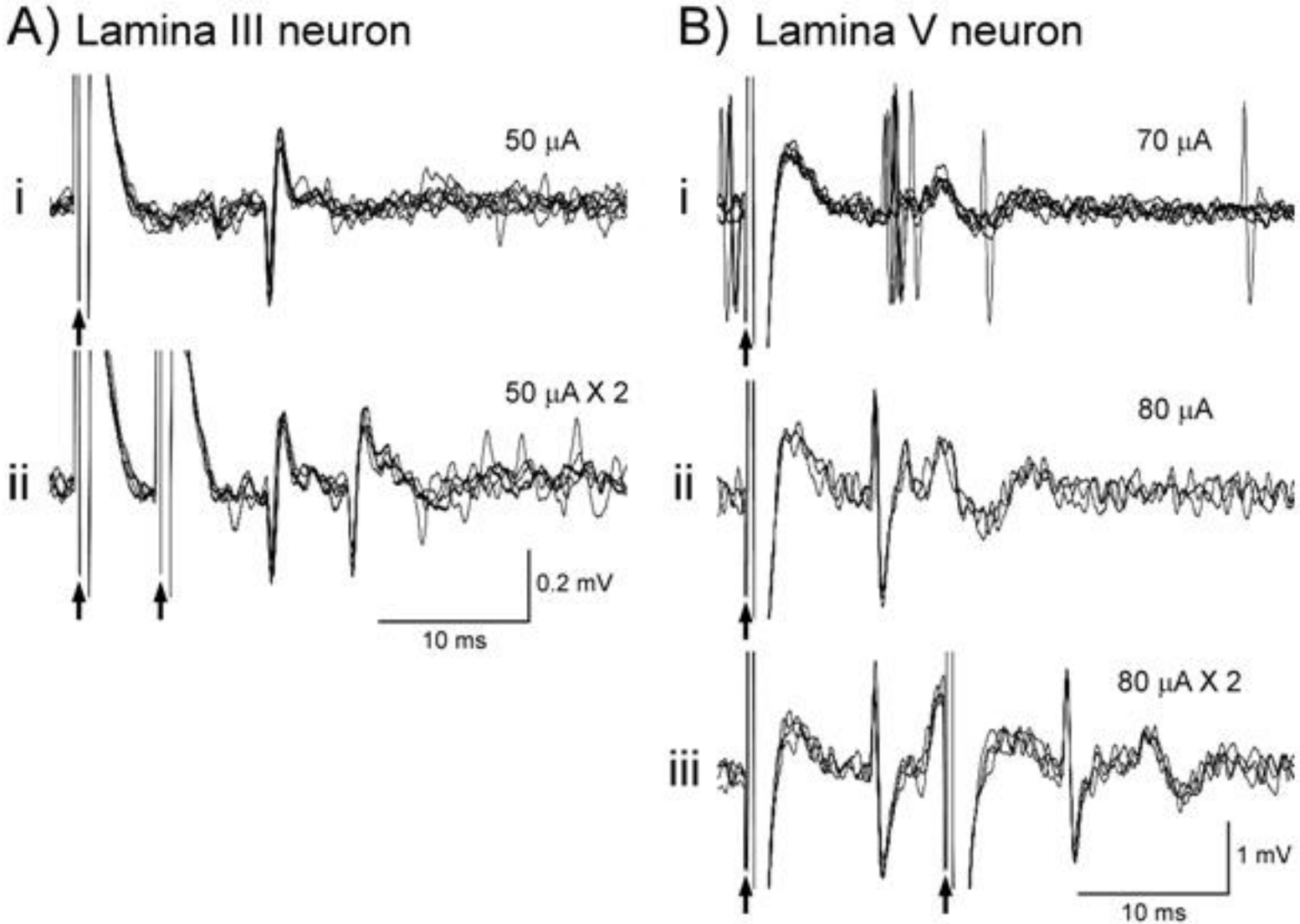

Fig.3 Bando Y. et al.

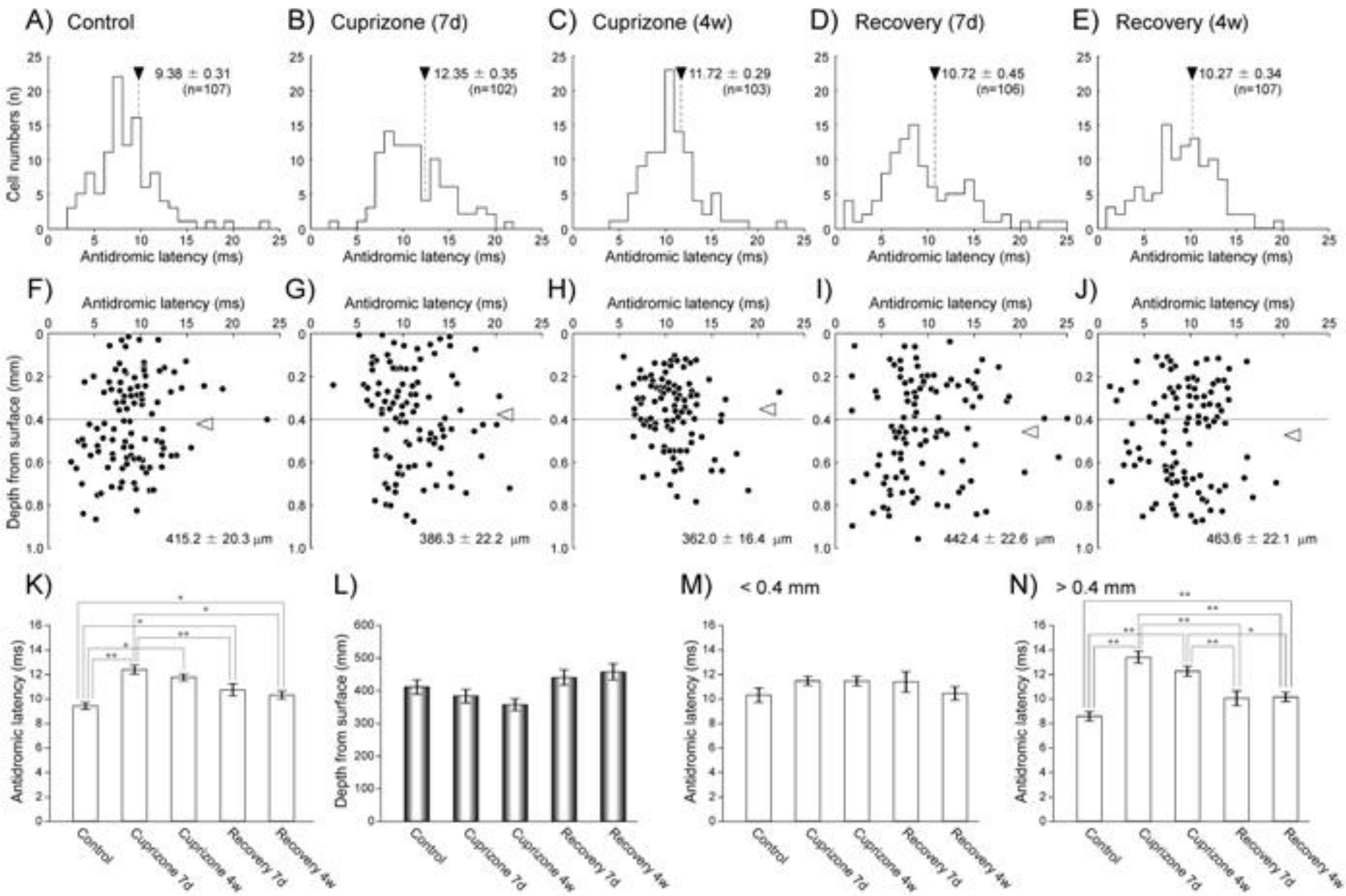

Fig.4 Bando Y et al.

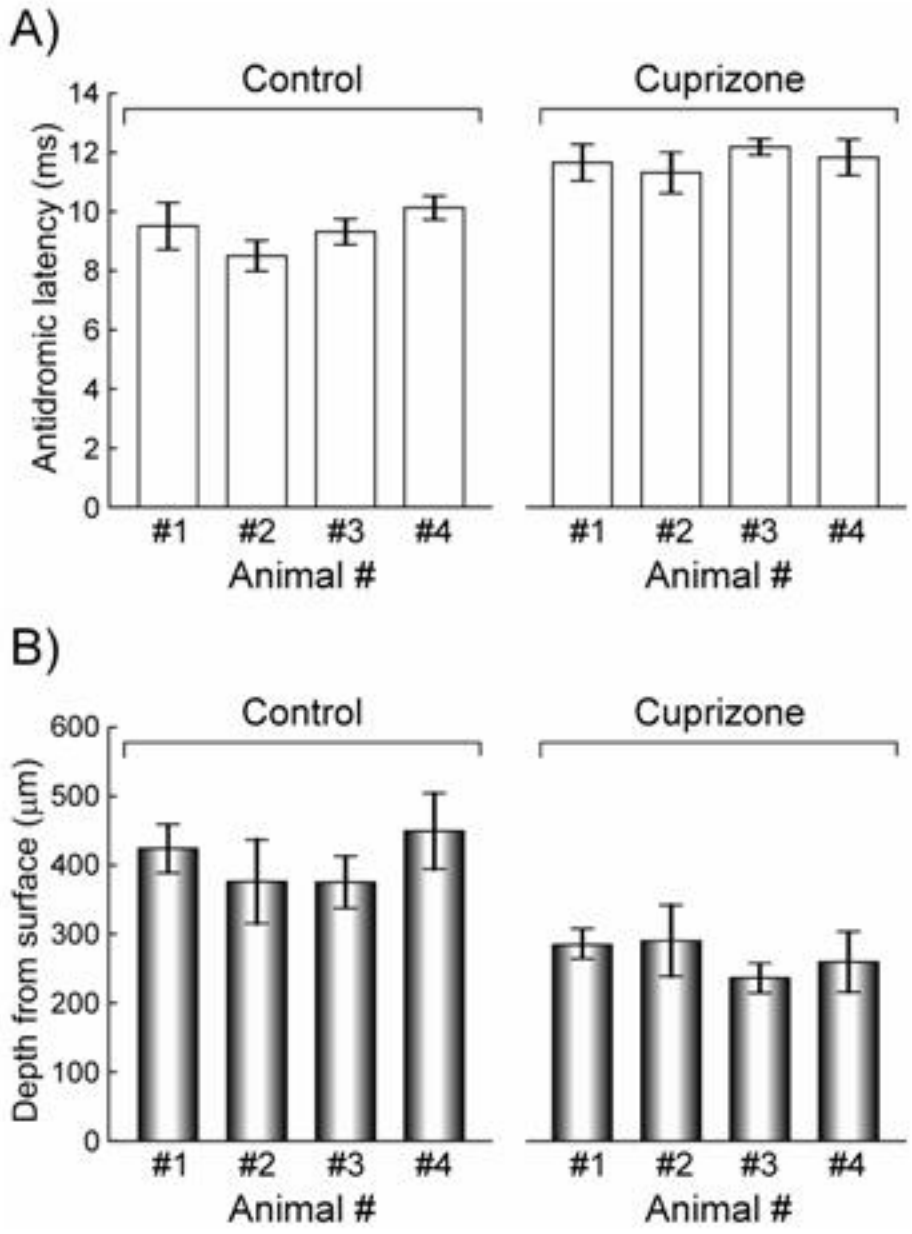

Fig.5 Bando Y et al.

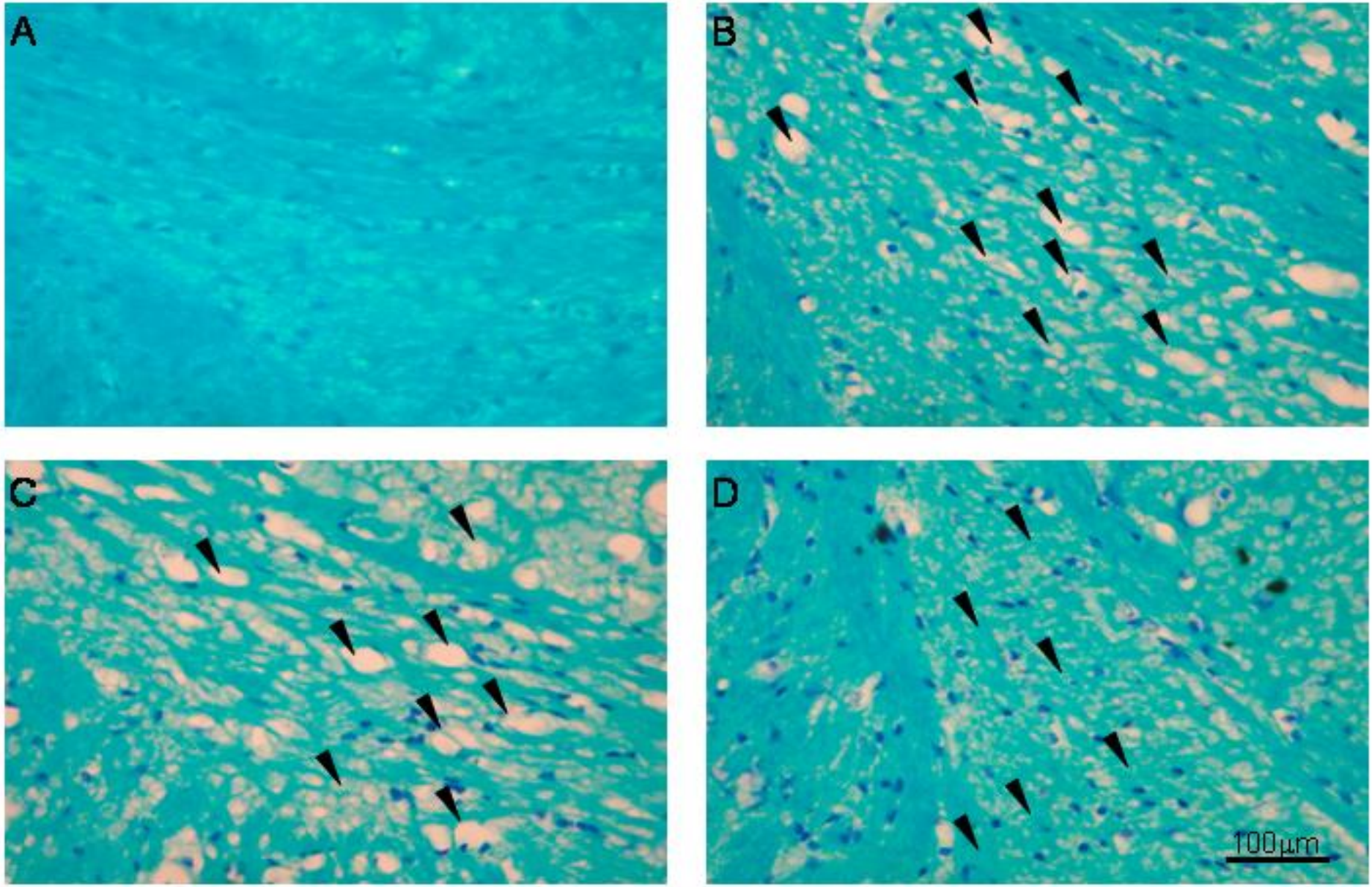

Fig.6 Bando Y. et al.

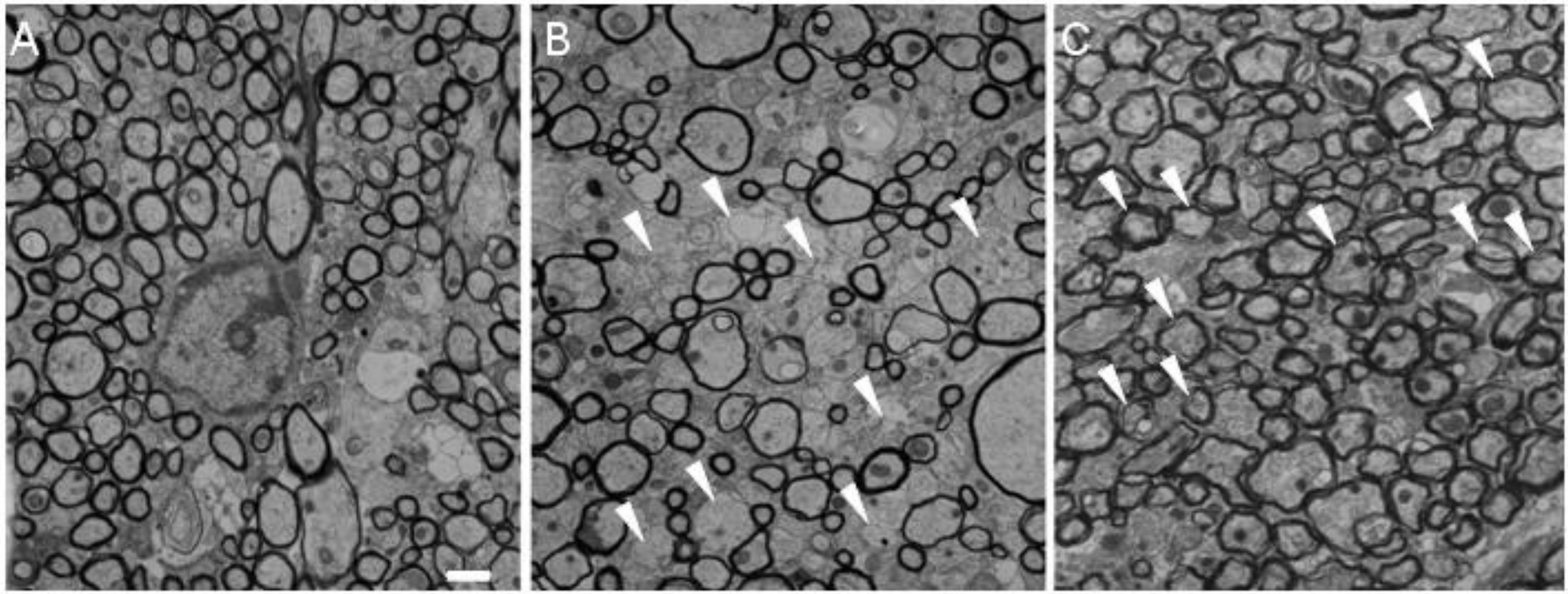

Fig.7 Bando Y et al.

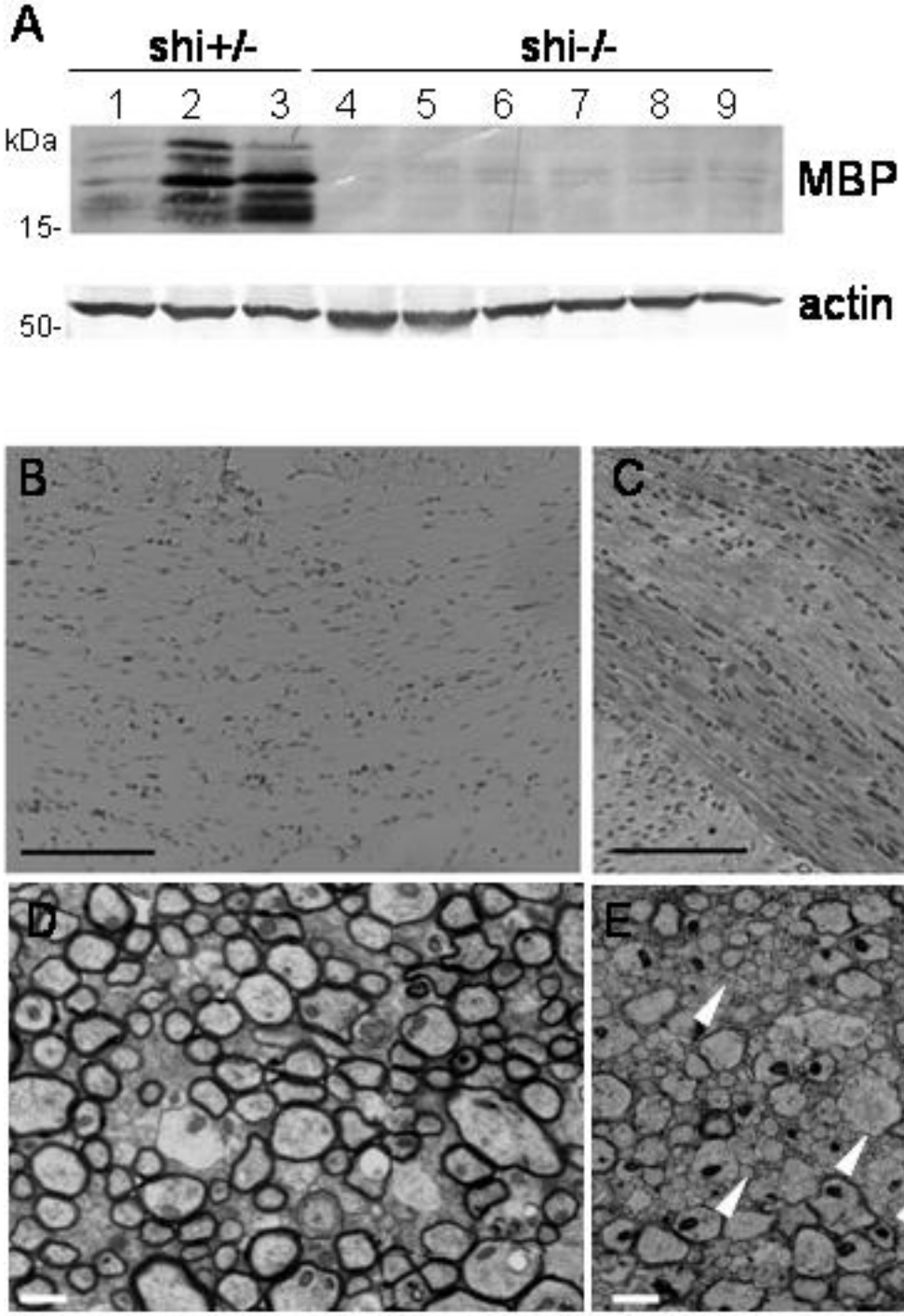

Fig.8 Bando Y. et al.

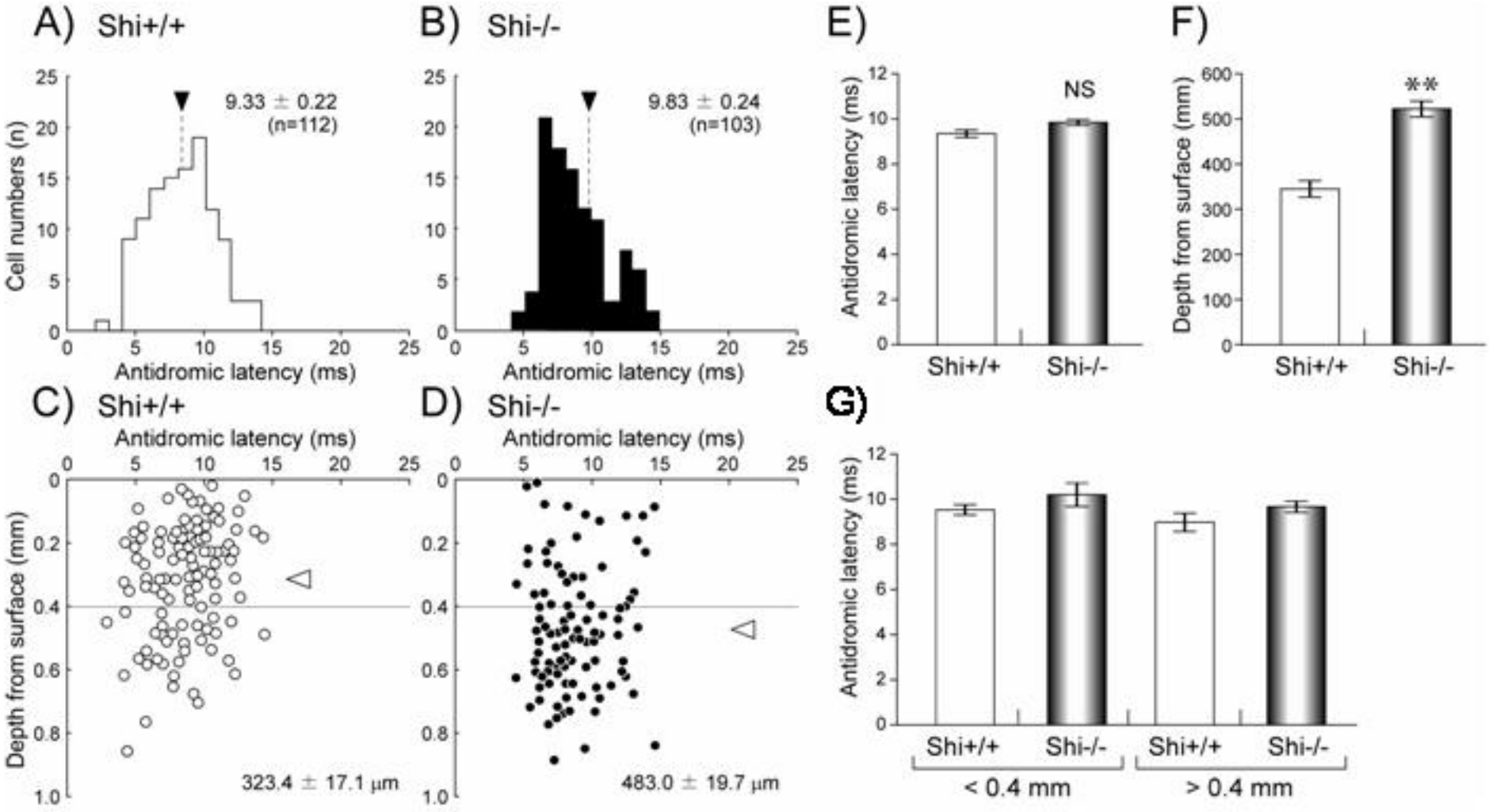

Fig.9 Bando Y et al.